Dalton Transactions

Accepted Manuscript

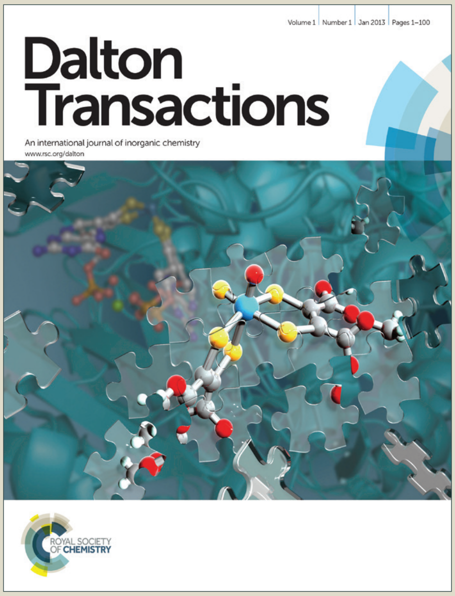

ROYAL SOCIETY OF CHEMISTRY

www.rsc.org/dalton

Journal Name RSCPublishing

COMMUNICATION

Cite this: DOI: 10.1039/x0xx00000x

Significantly Enhanced Dehydrogenation Properties of Calcium Borohydride Combined with Urea

Hailiang Chu,*[a] Shujun Qiu,[a] Lin Liu,[b] Yongjin Zou,[a] Cuili Xiang,[a] Huanzhi Zhang,[a] Fen Xu,[a] Lixian Sun,[a] Huaiying Zhou[a] and Guotao Wu *[b]

Received 00th January 2012,
Accepted 00th January 2012

DOI: 10.1039/x0xx00000x

www.rsc.org/

Interaction of [BH_x]- and [NH_x]-containing species gives rise of molecular hydrogen and the establishment of B-N bond. Up to now, Metal amides and ammonia are the commonly used [NH_x] sources. Herein, urea, an organic carbonyl diamide, was applied to react with $Ca(BH_4)_2$. A new type of complex hydrides $Ca(BH_4)_2$•$4CO(NH_2)_2$ was synthesized with releasing of *ca.* 5.2 wt.% hydrogen below 250 °C.

The development of hydrogen storage materials with high hydrogen content is of significant importance for the implementation of hydrogen fuel cell technology. $Ca(BH_4)_2$, with a hydrogen capacity of 11.4 wt.% and a favorable thermodynamics, has been considered as one of the promising hydrogen storage materials.[1] Extensive investigations have been carried out on this complex hydride in recent years. However, $Ca(BH_4)_2$ has to be heated to a temperature above 350 °C to release hydrogen, which is too high to be in practical application. In addition, the dehydrogenation is kinetically sluggish even at elevated temperatures.[2-3] Recent activities are somehow focusing on the thermodynamic and kinetic improvements of this compound through the additions of TiO_2,[4] disordered mesoporous carbon,[5] MgF_2,[6] transition metal fluorides,[7] Ti- or Nb-containing catalysts[8] and nanoscaffolds[9] etc.. In 2012, a ternary hydrogen storage system, $Ca(BH_4)_2$-$2LiBH_4$-$2MgH_2$, was developed with superior long-term cycling performance in the temperature range of 320 to 370 °C.[10]

An earlier work on the interaction of $LiNH_2$-LiH introduced a strategy to design possible hydrogen storage candidates, that is, facile dehydrogenation can result from the combination of protic H ($H^{\delta+}$) and hydridic H ($H^{\delta-}$).[11-12] Recently, unceasing research efforts led to the development of hydrogen storage systems comprising metal amides and calcium borohydrides.[13-18] Ball milling the mixtures of $Ca(BH_4)_2$ and $LiNH_2$ with variable $LiNH_2/Ca(BH_4)_2$ molar ratios results in different dehydrogenation properties.[13-14] For example, $Ca(BH_4)_2/4LiNH_2$ is capable of releasing more than 9 wt% of hydrogen in the temperature range of 250-350 °C, which show better dehydrogenation performances than pristine $Ca(BH_4)_2$.[14] With the assistance of nanosized Co catalyst, more than 4.5 and 7 wt.% of hydrogen can be released from $Ca(BH_4)_2/4LiNH_2$ sample at a temperature as low as 165 and 178 °C, respectively.[15] From theoretical calculations, the existence of a new quaternary compound, $CaBNH_6$, whose stoichiometry comes from a 1:1 mixture of $Ca(BH_4)_2$ and $Ca(NH_2)_2$, was predicted and its thermodynamically preferred decomposition reaction involves the formation of BN with a low decomposition enthalpy.[16] However, our experimental results show that ball milling the mixture of $Ca(BH_4)_2$ and $2Ca(NH_2)_2$ gives a mixture of solid products with poor crystallinity.[17] $Ca(BH_4)_2{\cdot}nNH_3$ complexes can produced hydrogen through the interaction of the protic H(N) of NH_3 with hydridic H(B) of $Ca(BH_4)_2$, and 11.3 wt.% of hydrogen could be released from $Ca(BH_4)_2{\cdot}2NH_3$ in closed reactor in the temperature range of 180 to 500 °C without the assistance of any catalysts.[19] Combination of $Ca(BH_4)_2{\cdot}NH_3$ with $LiBH_4$ was employed to advance its dehydrogenation, which showed tremendous suppression of ammonia formation and more than 12 wt.% H_2 release below 250 °C with favorable kinetics.[20] More than 10.0 wt.% H_2 can be released from $Ca(BH_4)_2/[C(NH_2)_3][BH_4]$ complex below 300 °C due to the combination of protic $H^{\delta+}$ (NH) and hydridic $H^{\delta-}$ (BH) hydrogens in the complex.[21] In these cases, the strong potential in the combination of protic $H^{\delta+}$ (NH) and hydridic $H^{\delta-}$ (BH) atoms and the establishment of a strong B-N bond should be one of the driving forces for the favorable dehydrogenation of these B-N-H composites. Although metal amides and ammonia have been be used for the modification of $Ca(BH_4)_2$, further improvements in dehydrogenation temperature, purity of gas released, etc. are still required.

Urea is an organic compound with the chemical formula $CO(NH_2)_2$. The molecule has two $-NH_2$ groups joined by a carbonyl (C=O) functional group. Urea is a non-toxic low-cost industrial product which is widely used as fertilizer. It can be synthesized from ammonia and CO_2 in large quantities. Urea, which has a gravimetric hydrogen content of 6.7 wt.%, is a promising, low cost, and reliable chemical hydride for hydrogen storage in transport applications.

Despite the benefits of using urea as a hydrogen carrier, there is little activity in converting urea to hydrogen.[22]

Herein, we demonstrate an effective approach for improving dehydrogenation properties of $Ca(BH_4)_2$ by interacting it with $CO(NH_2)_2$. By ball milling of $Ca(BH_4)_2$ and $CO(NH_2)_2$, a new complex with a chemical composition of $Ca(BH_4)_2 \cdot 4CO(NH_2)_2$ was synthesized. $Ca(BH_4)_2 \cdot 4CO(NH_2)_2$ complex shows substantially different dehydrogenation properties with respect to $Ca(BH_4)_2$, and 5.2 wt.% of hydrogen can be released in a stepwise manner starting at 100 °C.

Negligible amount of gaseous product was detected in the sample vessel after ball milling the mixtures with varying initial ratios of $Ca(BH_4)_2$ and $CO(NH_2)_2$ at 100 rpm for 2 h. XRD measurement on the powdery residue in molar ratio of 1:4 collected at the end of ball milling evidenced the disappearance of starting chemicals, i.e., $Ca(BH_4)_2$ and $CO(NH_2)_2$ (Fig. 1 and Fig. S1). A new set of diffraction peaks appears, which does not match with any known compound that contains elemental lithium, boron, nitrogen, oxygen, and hydrogen, and indicates the formation of a new complex of $Ca(BH_4)_2 \cdot 4CO(NH_2)_2$ by solid reaction between $Ca(BH_4)_2$ and $CO(NH_2)_2$ through the reaction.

$$Ca(BH_4)_2 + 4CO(NH_2)_2 \rightarrow Ca(BH_4)_2 \cdot 4CO(NH_2)_2 \quad (1)$$

Figure 1

Fig. 1 XRD patterns of (a) $CO(NH_2)_2$, (b) $Ca(BH_4)_2 \cdot 4CO(NH_2)_2$, and (c) $Ca(BH_4)_2$.

A range of experimental evidence has been obtained to support the assignment of the newly synthesized crystalline phase to $Ca(BH_4)_2 \cdot 4CO(NH_2)_2$. But our preliminary study using a combination of XRD analysis and first-principles calculations to solve its crystal structure is unsuccessful. As a complex containing *ca.* 7.74 wt.% hydrogen, $Ca(BH_4)_2 \cdot 4CO(NH_2)_2$ is a potential candidate for storing hydrogen. Temperature-programmed desorption coupled with mass spectroscopy (TPD-MS) profiles of $Ca(BH_4)_2 \cdot 4CO(NH_2)_2$, $CO(NH_2)_2$ and $Ca(BH_4)_2$ are shown in Fig. 2. The onset dehydrogenation temperature for $Ca(BH_4)_2 \cdot 4CO(NH_2)_2$ was as low as *ca.* 100 °C, which is about 160 °C lower than that of $Ca(BH_4)_2$. $Ca(BH_4)_2 \cdot 4CO(NH_2)_2$ releases hydrogen in a stepwise manner. Two sharp peaks at 125 and 210 °C, which is accompanied with a trace of ammonia signal for the second hydrogen evolution peak (Fig. 2 (a)). For the self-decomposition of $CO(NH_2)_2$, no H_2 signal and only NH_3 can be detected in the temperature range of 160 to 250 °C (Fig. 2 (a)). It is worthy of noting that side products, such as diborane, CO, CO_2, and HCNO were undetectable in the gaseous products of $Ca(BH_4)_2 \cdot 4CO(NH_2)_2$ in the temperature range of 30-500 °C. The dehydrogenation property of $Ca(BH_4)_2 \cdot 4CO(NH_2)_2$ exhibits remarkable difference from that of $Ca(BH_4)_2$, and the majority of hydrogen can be evolved at temperatures below 250 °C. Chemical bonding between B and N will be resulted after removal of hydrogen through the combination of $H^{\delta+}(NH_2)$ and $H^{\delta-}(BH_4)$. It is, therefore, difficult to re-hydrogenate the dehydrogenated products. To quantitatively measure hydrogen desorption from $Ca(BH_4)_2 \cdot 4CO(NH_2)_2$, a volumetric release test was performed. As shown in Fig. 2 (b), *ca.* 8 equiv. or 5.2 wt.% of H_2 can be released after holding the sample at 250 °C for 1 h according to the reaction (2). $Ca(BH_4)_2$, on the other hand, releases little H_2 when holding it at the same temperature (Fig. S2).

$$Ca(BH_4)_2 + 4\ CO(NH_2)_2 \rightarrow 8\ H_2 + [CaB_2C_4O_4N_8H_8] \quad (2)$$

Figure 2 (a)

Figure 2 (b)

Fig. 2 (a) TPD-MS and of H_2 (m/z=2), B_2H_6 (m/z=26) and NH_3 (m/z=16) of $Ca(BH_4)_2 \cdot 4CO(NH_2)_2$, $CO(NH_2)_2$ and $Ca(BH_4)_2$; (b) Time dependence of hydrogen desorption from $Ca(BH_4)_2 \cdot 4CO(NH_2)_2$. Sample was heated to 250 °C at a ramping rate of 2 °C min^{-1} and kept at 250 °C for 1 h.

Figure 3

Fig. 3 ^{11}B NMR spectra of (a) $Ca(BH_4)_2 \cdot 4CO(NH_2)_2$, (b) post-dehydrogenated and (c) $^1H \rightarrow {}^{11}B$ cross polarization $Ca(BH_4)_2 \cdot 4CO(NH_2)_2$ samples collected at 250 °C, (d) pristine $Ca(BH_4)_2$.

To further understand the decomposition process for $Ca(BH_4)_2 \cdot 4CO(NH_2)_2$ complex, characterizations on the solid products collected at 250 °C were performed. XRD measurement shows that the dehydrogenated samples are amorphous in nature (Fig. S3). Fig. 3 shows that solid ^{11}B NMR characterization on $Ca(BH_4)_2 \cdot 4CO(NH_2)_2$ complex reveals a single boron signal at $\delta = -35.9$ ppm which has a slightly upfield shift as compared with that of $Ca(BH_4)_2$ ($\delta = -29.8$ and 32.7 ppm for α- and β-phase, respectively). FT-IR characterization on $Ca(BH_4)_2 \cdot 4CO(NH_2)_2$ revealed that both the B-H stretching band in the region between 2500 cm^{-1} and 2000 cm^{-1} and the BH_2 deformation band at 1195 cm^{-1} and the characteristic N-H stretching band in the region between 2600 cm^{-1} and 3000 cm^{-1} and the NH_2 bending at 1469 cm^{-1} were detectable (Fig. S4). The post-250 °C dehydrogenated sample contains B species with resonances at around -36.8, -3.2, 16.6 and 22.5 ppm, respectively (Fig. 3). Although the peak is not obvious, B with a chemical shift at around -36.8 ppm should correspond to the residual BH_4^- species, which agrees with the fact that the B-H and N-H stretching bands can still be observed in FT-IR results (Fig. S4). Usually, chemical shift ranges from 0 to 40 ppm corresponds to tricoordinated B^{III} atoms, and chemical shift ranges from -40 to 0 ppm corresponds to tetracoordinated B^{IV} atoms.[23-24] The broad resonances centered around -3.2 ppm may be assigned to the tetravalent BN_3 or NBH_2 species, respectively,[23-24] but the presence of BO_2 group (chemical shift of 1.3±0.5 ppm) and tetragonal BO_4 group (chemical shift of 0.7 ppm) in the dehydrogenated product could not be excluded,[25] which needs further characterization. The ^{11}B MAS NMR spectrum of the sample treated at 250 °C also presents a broad lineshape with two overlapping ^{11}B peaks, at 16.6 and 22.5 ppm, which may be assigned to the trivalent HN-B=N species. $^1H \rightarrow {}^{11}B$ cross polarization NMR measurement shows that tetravalent borane hydrogen substances (chemical shift of -36.4 ppm), tetravalent borane nitrogen substances (chemical shift of -2.9 ppm), and triavalent borane nitrogen substances (chemical shift of 23.9 ppm) carry hydrogen atoms. According to the ^{11}B NMR and FT-IR results, the dehydrogenation mechanism of $Ca(BH_4)_2 \cdot 4CO(NH_2)_2$ complex may be similar to that of other B-N-H systems, i.e. hydrogen release from $Ca(BH_4)_2 \cdot 4CO(NH_2)_2$

complex may result from the dissociation of both B-H bonds of $Ca(BH_4)_2$ and N-H bonds of $CO(NH_2)_2$ followed by the combination of B and N.[26-33] The formation of $Ca(BH_4)_2{\cdot}4CO(NH_2)_2$ complex results in close contact between H(B) and H(N), so that the combination of B-H and N-H proceeds easily and leads to H_2 release at much lower temperatures. Furthermore, the combination of B and N can remarkably suppress the release of NH_3 from $Ca(BH_4)_2{\cdot}4CO(NH_2)_2$ complex and lead to a relatively pure gaseous product.

Conclusions

In summary, a new $Ca(BH_4)_2{\cdot}4CO(NH_2)_2$ complex can be formed by solid reaction of $CO(NH_2)_2$ with $Ca(BH_4)_2$ in a molar ratio of 1:4. 5.2 wt.% of hydrogen can be released from $Ca(BH_4)_2{\cdot}4CO(NH_2)_2$ complex at reduced temperatures, which enables this new material a promising candidate for hydrogen storage. Interaction of N-H and B-H in $Ca(BH_4)_2{\cdot}4CO(NH_2)_2$ complex is the key factor for improving the dehydrogenation. Further investigations are needed to understand the reaction mechanism and to enhance the dehydrogenation kinetics of $Ca(BH_4)_2{\cdot}4CO(NH_2)_2$ complex. It is worthy of highlighting that the present work may open a door in exploring organic-inorganic hybrid system for hydrogen storage.

Acknowledgements

This work was financially supported by the Ministry of Science and Technology of China (2010CB631303), the National Natural Science Foundation of China (51101144, 51461010, 51401059, 51361005, 51201041, 51371060, 21173111, 51361006, 51201042, and 51102230), Guangxi Natural Science Foundation (2013GXNSFBA019034, 2013GXNSFBA019239, 2014GXNSFAA118043, 2014GXNSFAA118333) and Guangxi University Research Project (2013ZD023, YB2014132).

Notes and references

[a] *School of Materials Science and Engineering, Guilin University of Electronic Technology, No. 1, Jinji Road, Guilin 541004, PR China*
E-mail: chuhailiang@guet.edu.cn; Fax: +86-411-2290129; Tel.: +86-773-2216607.
[b] *Dalian Institute of Chemical Physics, Chinese Academy of Sciences, No. 457, Zhongshan Road, Dalian 116023, PR China*
E-mail: wgt@dicp.ac.cn

† Electronic Supplementary Information (ESI) available: Experimental details; XRD patterns of $Ca(BH_4)_2$-$CO(NH_2)_2$ in different molar ratios; Volumetric release of pristine $Ca(BH_4)_2$ at 250 °C; XRD patterns of post-dehydrogenated $Ca(BH_4)_2{\cdot}4CO(NH_2)_2$ at different temperatures; FT-IR results. See DOI: 10.1039/c000000x/

1 K. Miwa, M. Aoki, T. Noritake, N. Ohba, Y. Nakamori, S. Towata, A. Züttel, and S. Orimo, *Phys. Rev. B*, 2006, **74**, 155122.

2 H. W. Li, Y. G. Yan, S. Orimo, A. Zuttel and C. M. Jensen, *Energies*, 2011, **4**, 185-214.

3 C. B. Minella, E. Pellicer, E. Rossinyol, F. Karimi, C. Pistidda, S. Garroni, C. Milanese, P. Nolis, M. D. Baro and O. Gutfleisch, *J. Phys. Chem. C*, 2013, **117**, 4394-4403.

4 J. Gu, M. X. Gao, H. G. Pan, Y. F. Liu, B. Li, Y. J. Yang, C. Liang, H. L. Fu and Z. X. Guo, *Energy Environ. Sci.*, 2013, **6**, 847-858.

5 A. Ampoumogli, T. Steriotis, P. Trikalitis, E. G. Bardaji, M. Fichtner, A. Stubos and G. Charalambopoulou, *Int. J. Hydrogen Energy*, 2012, **37**, 16631-16635.

6 R. Gosalawit-Utke, K. Suarez, J. M. B. von Colbe, U. Bosenberg, T. R. Jensen, Y. Cerenius, C. B. Minella, C. Pistidda, G. Barkhordarian and M. Schulze, *J. Phys. Chem. C*, 2011, **115**, 3762-3768.

7 C. B. Minella, S. Garroni, C. Pistidda, R. Gosalawit-Utke, G. Barkhordarian, C. Rongeat, I. Lindemann, O. Gutfleisch, T. R. Jensen and Y. Cerenius, *J. Phys. Chem. C*, 2011, **115**, 2497-2504.

8 J. H. Kim, J. H. Shim and Y. W. Cho, *J. Power Sources*, 2008, **181**, 140-143.

9 C. Comanescu, G. Capurso and A. Maddalena, *Nanotechnology*, 2012, **23**, 385401.

10 M. X Gao, J. Gu, H. G. Pan, Y. L. Wang, Y. F. Liu, C. Liang and Z. X. Guo, *J. Mater. Chem.*, 2012, **22**, 5312-5318.

11 P. Chen, Z. T. Xiong, J. Z. Luo, J. Y. Lin and K. L. Tan, *Nature*, 2002, **420**, 302-304.

12 P. Chen, Z. T. Xiong, J. Z. Luo, J. Y. Lin and K. L. Tan, *J. Phys. Chem. B*, 2003, **107**, 10967-10970.

13 H. L. Chu, Z. T. Xiong, G. T. Wu, J. P. Guo, T. He and P. Chen, *Dalton Trans.*, 2010, **39**, 10585-10587.

14 H. L. Chu, Z. T. Xiong, G. T. Wu, J. P. Guo, X. L Zheng, T. He, C. Z. Wu and P. Chen, *Chem. -Asian J.*, 2010, **5**, 1594-1599.

15 H. L. Chu, S. J. Qiu, L. X. Sun and G. T. Wu, *J. Renewable Sustainable Energy*, 2014, **6**, 013105.

16 D. S. Aidhy, Y. S. Zhang and C. Wolverton, *Phys. Rev. B*, 2011, **84**, 134103.

17 H. L. Chu, G. T. Wu, Y. Zhang, Z. T. Xiong, J. P. Guo, T. He and P. Chen, *J. Phys. Chem. C*, 2011, **115**, 18035-10841.

18 X. B. Yu, Z. X. Yang, Y. H. Guo and S. G. Li, *J. Alloys Compd.*, 2011, **509**, S724-S727.

19 H. L. Chu, G. T. Wu, Z. T. Xiong, J. P. Guo, T. He and P. Chen, *Chem. Mater.*, 2010, **22**, 6021-6028.

20 Z. W. Tang, Y. B. Tan, Q. F. Gu and X B. Yu, *J. Mater. Chem.*, 2012, **22**, 5312-5318.

21 Z. W Tang, Y. H. Guo, S. F. Li and X. B. Yu, *J. Phys. Chem. C*, 2011, **115**, 3188-3193.

22 A. N. Rollinson, J. Jones, V. Dupont and M. V. Twigg, *Energy Environ. Sci.*, 2011, **4**, 1216-1224.

23 C. Gervais, J. Maquet, F. Babonneau, C. Duriez, E. Framery, M. Vaultier, P. Florian and D. Massiot, *Chem. Mater.*, 2001, **13**, 1700-1707.

24 A. Doroodian, J. E. Dengler, A. Genest, N. Rosch and B. Rieger, *Angew. Chem., Int. Ed.*, 2010, **49**, 1871-1873.

25 G. D. Soraru, N. Dallabona, C. Gervais and F. Babonneau, *Chem. Mater.*, 1999, **11**, 910-919.

26 Z. T. Xiong, C. K. Yong, G. T. Wu, P. Chen, W. Shaw, A. Karkamkar, T. Autrey, M. O. Jones, S. R. Johnson, P. P. Edwards and W. F. David, *Nat. Mater.*, 2008, **7**, 138-141.

27 H. Wu, W. Zhou and T. Yildirim, *J. Am. Chem. Soc.*, 2008, **130**, 14834-14839.

28 X. D. Kang, Z. Z. Fang, L. Y. Kong, H. M. Cheng, X. D. Yao, G. Q. Lu and P. Wang, *Adv. Mater.*, 2008, **20**, 2756-2759.

29 T. J. Groshens and R. A. Hollins, *Chem. Commun.*, 2009, **21**, 3089-3091.

30 T. Hügle, M. F. Kühnel and D. Lentz, *J. Am. Chem. Soc.*, 2009, **131**, 7444-7446.

31 G. Soloveichik, J. Her, P. W. Stephens, Y. Gao, J. Rijssenbeek, M. Andrus and J. C. Zhao, *Inorg. Chem.*, 2008, **47**, 4290-4298.

32 Y. H. Guo, X. B. Yu, W. W. Sun, D. L. Sun and W. N. Yang, *Angew. Chem., Int. Ed.*, 2011, **50**, 1087-1091.

33 Z. G. Huang, J. Gallucci, X. N. Chen, T. Yisgedu, H. K. Lingam, S. G. Shore and J. C. Zhao, *J. Mater. Chem.*, 2010, **20**, 2743-2745.

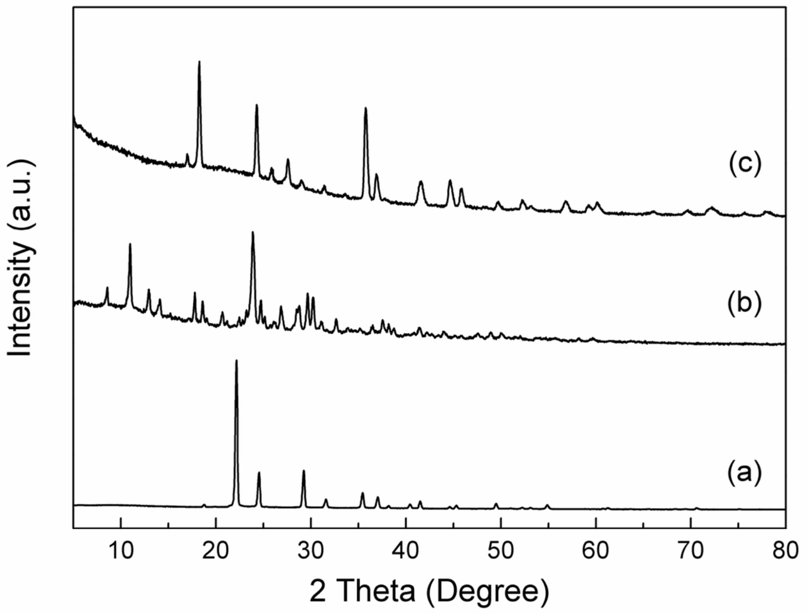

127x89mm (300 x 300 DPI)

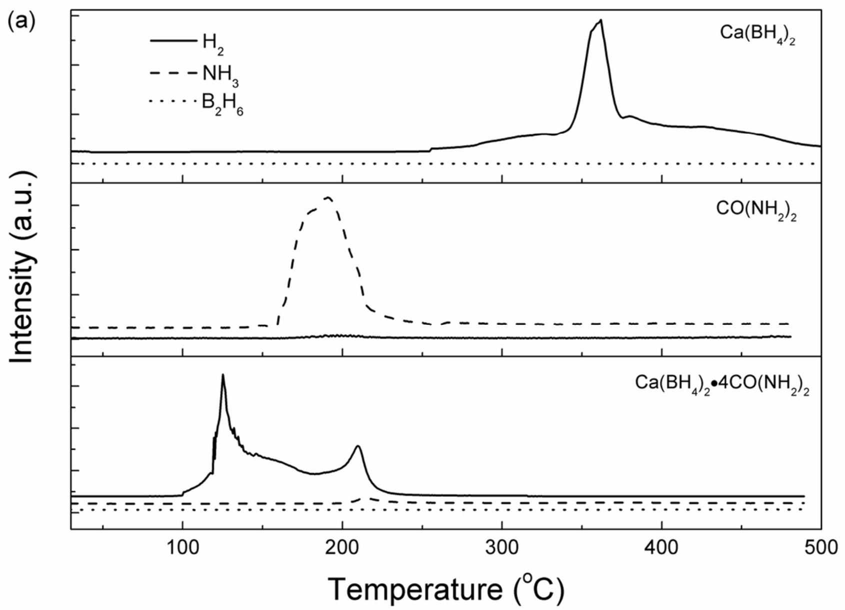

121x81mm (300 x 300 DPI)

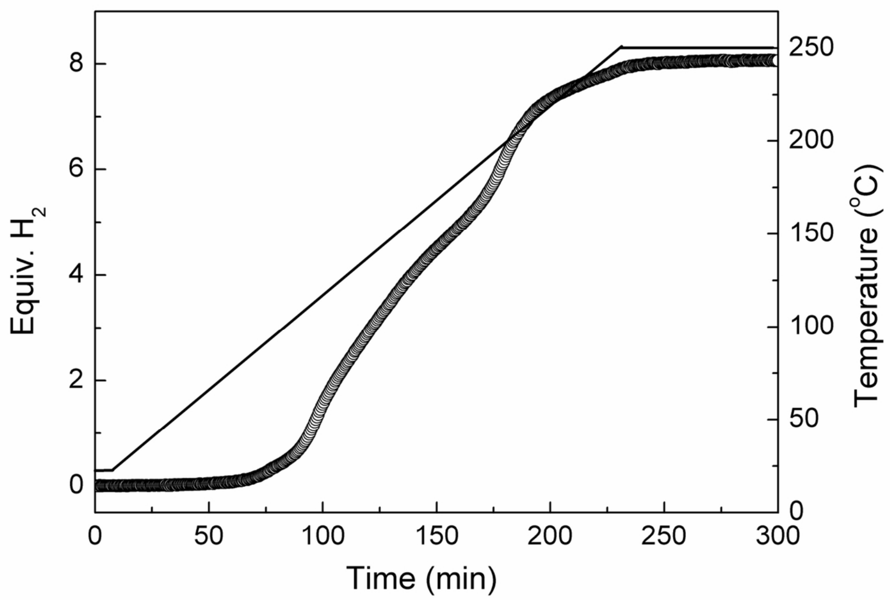

127x89mm (300 x 300 DPI)

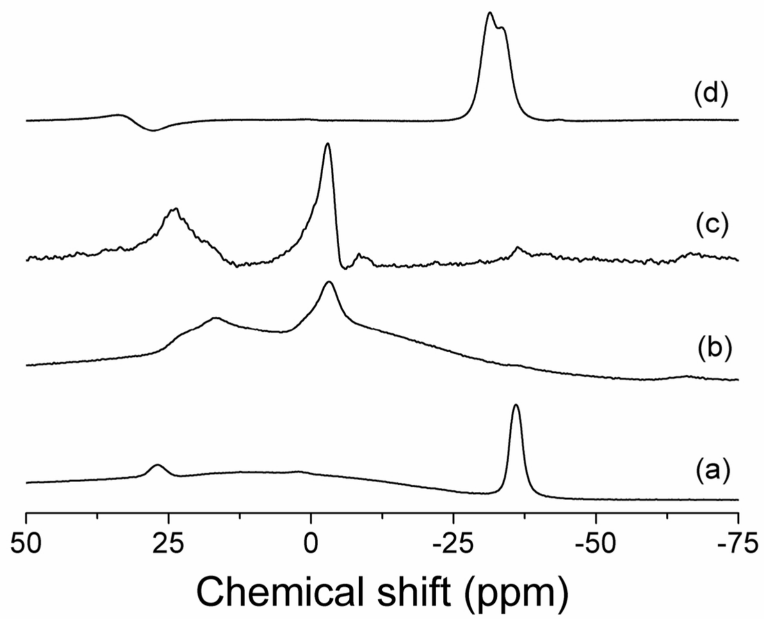

127x89mm (300 x 300 DPI)